

## Anomalous properties of the $\text{Yb}_x\text{Y}_{1-x}\text{InCu}_4$ alloy system

M. Očko,<sup>1,\*</sup> J. L. Sarrao,<sup>2</sup> I. Aviani,<sup>1</sup> Dj. Drobac,<sup>1</sup> I. Živković,<sup>1</sup> and M. Prester<sup>1</sup>

<sup>1</sup>*Institute of Physics, P.O. Box 304, 10000, Zagreb, Croatia*

<sup>2</sup>*Los Alamos National Laboratory, Mail Stop K 764, Los Alamos, New Mexico 87545, USA*

(Received 24 December 2002; revised manuscript received 19 March 2003; published 6 August 2003)

We report on lattice parameter, dc and ac susceptibility, thermopower, and resistivity measurements of the  $\text{Yb}_x\text{Y}_{1-x}\text{InCu}_4$  alloy system. With increasing  $x$  the system evolves from semimetallic towards more metallic character. Some anomalous properties, such as the concentration dependence of the lattice parameter can be explained as an admixture of  $\text{Yb}^{+3}$  and  $\text{Yb}^{+2}$  ions. Only for the lowest concentrations of Yb do we observe signs of the Kondo effect with a  $T_K$  of about 2 K, which is much lower than expected. The absence of a signature of the Kondo effect in the thermopower data for the lowest concentrations we explain by the semimetallic character of the  $\text{YInCu}_4$  matrix. The valence transition is detected for  $x > 0.85$  by thermopower as well as by susceptibility and resistivity data.

DOI: 10.1103/PhysRevB.68.075102

PACS number(s): 72.15.Qm, 75.20.Hr, 72.15.Eb, 72.15.Jf

### I. INTRODUCTION

Many properties of  $\text{YbInCu}_4$ , a very interesting moderately heavy fermion (HF) compound, were discussed within the single ion theories based on the Kondo character of the  $\text{Yb}^{+3}$  ion.<sup>1-3</sup> The Kondo character of  $\text{Yb}^{+3}$  is expected from the electron-hole symmetry of the  $\text{Yb}^{+3}$  and  $\text{Ce}^{+3}$  ion, which is a Kondo ion.<sup>4</sup> Experimentally, the Kondo character of  $\text{Yb}^{+3}$  was observed, for example, in the transport properties of the heavy fermion compound  $\text{YbCu}_2\text{Si}_2$  under pressure.<sup>5</sup> In this and many other experiments the Yb ion shows a difference with respect to the Ce ion to the extent that with increasing pressure the Kondo temperature decreases. In contrast, the susceptibility data of the  $\text{Yb}_x\text{Y}_{1-x}\text{CuAl}$  alloy system show for each concentration a hump at about 25 K and a Curie-Weiss-like behavior at higher temperatures.<sup>6</sup> The concentration independency of the position of the hump in  $\text{Yb}_x\text{Y}_{1-x}\text{CuAl}$  is explained by the single ion description of the intermediate valence state.<sup>6</sup> However, it is not clear, if it was so, why the position is not moved due to the considerable change of the lattice parameter, as reported.

$\text{YbInCu}_4$  displays a first order valence transition separating its high- $T$  and low- $T$  phases.<sup>1-3</sup> The low- $T$  phase of  $\text{YbInCu}_4$  is characterized by enhanced Pauli susceptibility, which could be interpreted as one of the regimes of Kondo behavior—Kondo saturation. In this scenario one can estimate the Kondo temperature  $T_K(L) \approx 400$  K.<sup>1,3</sup> The thermopower measurements indicates also a high  $T_K(L)$ .<sup>7</sup> The linear coefficient of specific heat  $\gamma = 50$  mJ/mol K<sup>2</sup>, supports a view of the moderately heavy fermion character of the low-temperature phase.<sup>1,3</sup> The transport properties, resistivity and thermopower, of the low- $T$  phase were described within the same picture.<sup>7</sup>

The high- $T$  phase of  $\text{YbInCu}_4$  as well as  $\text{Yb}_x\text{Y}_{1-x}\text{InCu}_4$  alloy system is characterized by a Curie-Weiss-like susceptibility with small Curie-Weiss constant  $\theta \approx -5$  K and with an effective magnetic moment  $4.54/\text{Yb}$  that is 90% of the full multiplet of  $\text{Yb}^{+3}$  ( $g = 8/7$ ,  $J = 7/2$ ). The small reduction of the moment and the small antiferromagnetic constant  $\theta$  could

be ascribed to Kondo interaction with  $T_K \approx 25$  K.<sup>1-3</sup> It was believed that the most prominent feature of Kondo behavior in susceptibility data, Kondo saturation or even a hump, as in Ref. 6, was not observed because the system undergoes the isostructural first-order valence transition at  $T_V = 42$  K before the Kondo temperature could be reached. There are no clear signatures of the Kondo effect also in the transport properties of  $\text{YbInCu}_4$  in the high- $T$  phase. In our recent work we tried to reveal Kondo characteristics by chemically suppressing the valence transition.<sup>8</sup> In particular, the temperature of the valence transition  $T_V$  decreases by alloying  $\text{YbInCu}_4$  with Y.<sup>2</sup> Further, one expects an increase of  $T_K$  because the  $\text{Y}^{+3}$  is larger than  $\text{Yb}^{+3}$  ion (and chemical pressure should decrease  $T_K$  in Yb systems<sup>5</sup>). By tuning the valence transition to lower temperatures and increasing  $T_K$ , we expected to observe some signatures of the Kondo effect. The preliminary experiments did not prove our expectations and we did not observe clear Kondo signatures corresponding to  $T_K > 25$  K in the high temperature phase for  $x > 0.85$ .

The motivation for further investigations of the  $\text{Yb}_x\text{Y}_{1-x}\text{InCu}_4$  system was to investigate whether the Yb ion shows Kondo characteristics in the impurity limit. Again, we would expect much higher  $T_K$  than 25 K because the lattice parameter increases with decreasing  $x$ . In reviewing the existing literature, one finds that there are relatively few investigations, especially of transport properties, on alloy systems containing Yb, especially in the dilute limit—certainly many fewer than those on alloy systems containing Ce. Another interesting issue is the matrix  $\text{YInCu}_4$  in which the Yb ion is dissolved. Usually one finds investigations where Ce, Yb, and U are dissolved in a metal matrix with relatively broad conducting band. It was shown that  $\text{YInCu}_4$  matrix assumes semimetal characteristic and this fact makes the  $\text{Yb}_x\text{Y}_{1-x}\text{InCu}_4$  alloy system additionally interesting for investigation.<sup>9</sup>

### II. EXPERIMENTAL DETAILS

Details of sample preparations and experimental methods were described elsewhere.<sup>1,2,7</sup> Here, we add that our investi-

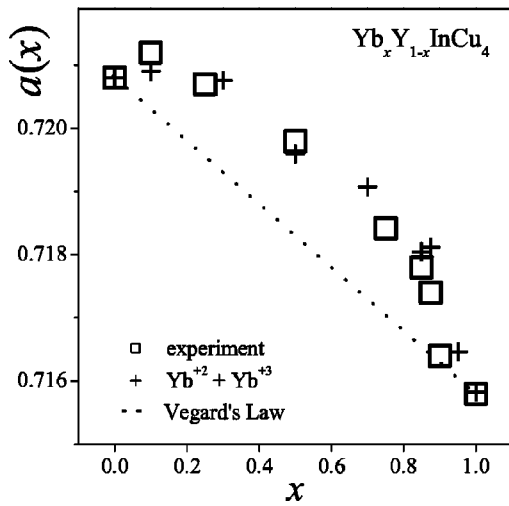


FIG. 1. The lattice parameter  $a$  of the  $\text{Yb}_x\text{Y}_{1-x}\text{InCu}_4$  alloy system (squares) versus concentration of the Yb ions  $x$ . The calculated values of  $a$  by the relation (2) are denoted by pluses.

gations are performed on monocrystals of the  $\text{Yb}_x\text{Y}_{1-x}\text{InCu}_4$  alloy system grown in an In-Cu flux. Various experimental investigations are performed on different samples, but from the same batch for a given concentration.

### III. EXPERIMENTAL RESULTS AND DISCUSSIONS

X-ray diffraction analysis for each concentration showed only the phase with a cubic  $C15b$  crystal structure ( $\text{MgCu}_4\text{Sn}$  type). The concentration dependence of the lattice constant  $a$  shown in Fig. 1 (open squares) does not follow Vegard's law. At first glance, it seems that there is a difference between actual and nominal concentration of the Yb ion in an alloy. However, a closer look at the data and the analysis of the susceptibility suggests another interpretation.

The dc susceptibility,  $\chi$  data of the  $\text{Yb}_x\text{Y}_{1-x}\text{InCu}_4$  alloy system are shown in Fig. 2 by presenting  $1/\chi$  versus temperature for various concentrations. We do not present all the investigated concentrations here for the sake of clarity. For

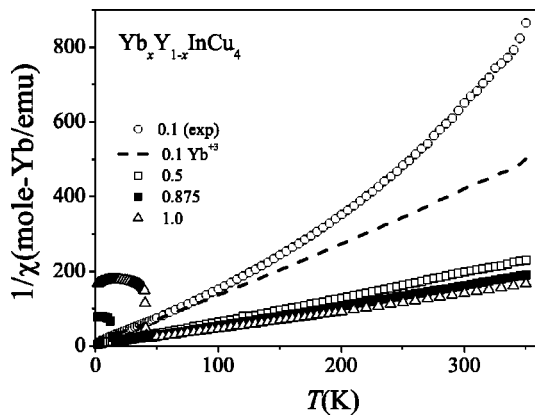


FIG. 2. The susceptibility data  $\chi$  shown as  $1/\chi$  of the  $\text{Yb}_x\text{Y}_{1-x}\text{InCu}_4$  alloy system versus temperature  $T$  for some selected concentrations. The dashed line for  $x=0.1$  represents the contribution of the  $\text{Yb}^{+3}$  ion.

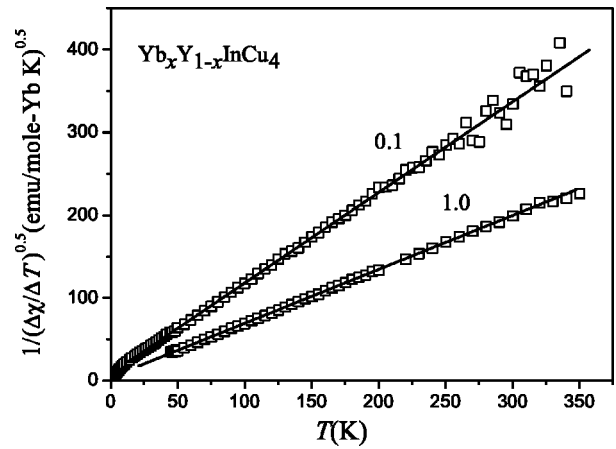


FIG. 3. Examples of the procedure used for the determination of the quantities in the expression (1) from the dc susceptibility data. See details in the text.

higher concentrations,  $x > 0.7$ , the raw data show a Curie-Weiss-like behavior at higher temperatures ( $x > 50$  K). For lower concentrations there is evident curvature in the data. After subtraction of a linear term, explained below, the data show Curie-Weiss-like behavior for lower concentrations as well. This is represented by the dotted line for  $x=0.1$ . For  $x \geq 0.875$  there is a jump in the  $1/\chi$  data due to the valence transition. In a simple analysis of susceptibility data of a paramagnetic system at higher temperatures one usually fits the data by the expression

$$\chi = C/(T + \theta) + \chi_0. \quad (1)$$

The first term represents the contribution of moment bearing ions and  $\chi_0$  represents matrix contribution. We differentiate the expression (1) and in Fig. 3 we plot  $[1/(\Delta\chi/\Delta T)]^{1/2}$  versus  $T$  for  $x=0.1$  and  $x=1.0$ . Above 50 K one observes expected linear behavior. From the parameters of this linear behavior it is easy to calculate the constants  $C$  and  $\theta$ . In Fig. 4 we plot  $\chi_0 = \chi_{\text{EXP}} - \chi_{\text{CW}}$ .  $\chi_0$  is constant within experimental error above 50 K. In the lower section of Fig. 5 we plot  $L = \chi_0(T > 50 \text{ K})$  versus  $x$ .  $L$  reveals a diamagnetic response. We note also that  $\text{YInCu}_4$ , represented by the line in Fig. 4, is a diamagnetic compound.  $L$  increases with  $x$ , which is apparently connected with the increase in the number of inner electrons resulting from the substitution of Yb for Y with increasing  $x$ . In the middle section of Fig. 5 we show  $\theta$  versus  $x$ , which is relatively independent of  $x$ . The most striking characteristic of the  $\text{Yb}_x\text{Y}_{1-x}\text{InCu}_4$  alloy system, which distinguishes it clearly from, for example,  $\text{Yb}_x\text{Y}_{1-x}\text{CuAl}$  is given in the upper section of Fig. 5. We plot  $C/C_{\text{th}}$  versus  $x$ , where  $C_{\text{th}}$  is the theoretical value of the Curie constant per mole  $\text{Yb}^{+3}$  and  $C$  is the extracted constant of an alloy calculated per mole Yb. For  $\text{Yb}_x\text{Y}_{1-x}\text{CuAl}$  this quantity is independent of  $x$  and about 1, as reported. This implies that the concentration of  $\text{Yb}^{+3}$ , i.e., the magnetic properties scales with concentration in  $\text{Yb}_x\text{Y}_{1-x}\text{CuAl}$ .

In order to explain the concentration dependence of the lattice parameter vs  $x$  in  $\text{Yb}_x\text{Y}_{1-x}\text{InCu}_4$  we assume that in an alloy there is a statistical mixture of  $\text{Yb}^{+3}$  and  $\text{Yb}^{+2}$ , i.e., a

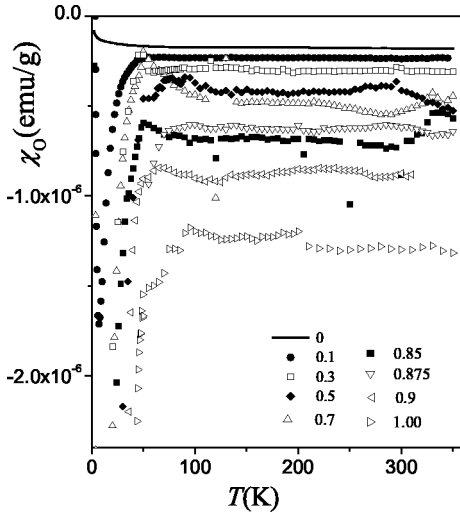


FIG. 4. Difference between the measured susceptibility  $\chi$  and the Curie-Weiss form of the susceptibility with the constant  $C$  and  $\theta$  determined by the procedure described in the text. The graph shows that the quantity  $\chi_0$  defined in the expression (1) is constant above about 50 K. The full line represents the susceptibility of  $\text{YInCu}_4$ .

mixed valence state, with concentrations  $C/C_{\text{th}}x$  and  $(1 - C/C_{\text{th}})x$ , respectively. Assuming this, we have calculated the lattice parameter from the expression (pluses in Fig. 1):

$$a(x) = xC/C_{\text{th}}a_{\text{Yb}^{+3}} + x(1 - C/C_{\text{th}})a_{\text{Yb}^{+2}} + (1-x)a_{\text{Y}}. \quad (2)$$

$a_{\text{Y}} = 0.7208$  nm is the experimentally determined lattice parameter of  $\text{YInCu}_4$ . We take  $a_{\text{Yb}^{+3}} = 0.7147$  nm as the lattice parameter of  $\text{YbInCu}_4$  containing  $\text{Yb}^{+3}$  only and  $a_{\text{Yb}^{+2}} = 0.72152$  nm as the lattice parameter of  $\text{YbInCu}_4$  containing  $\text{Yb}^{+2}$  only. The choice of  $a_{\text{Yb}^{+2}}$  and  $a_{\text{Yb}^{+3}}$

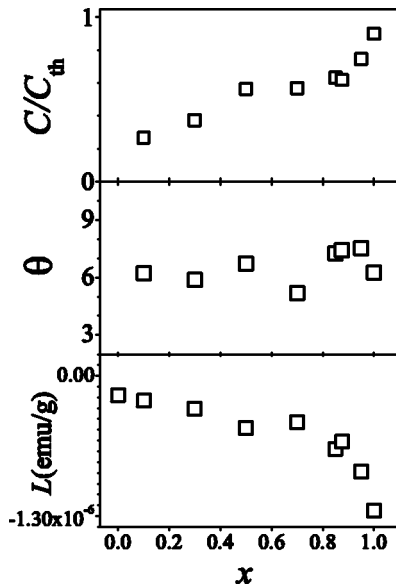


FIG. 5. Upper section:  $C/C_{\text{th}}$  versus  $x$ ;  $C_{\text{th}}$  is the theoretical value of the Curie constant per mole  $\text{Yb}^{+3}$  and  $C$  is the extracted constant of an alloy calculated per mole Yb. Middle section:  $\theta$  versus  $x$ . Lower section:  $L = \chi_0(T > 50 \text{ K})$  versus  $x$ .

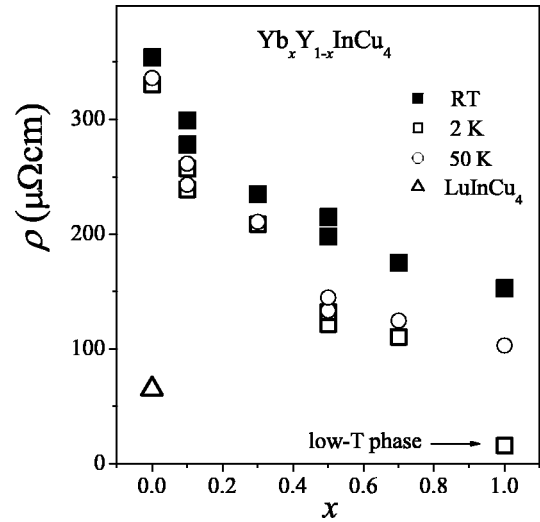


FIG. 6. The room temperature resistivity  $\rho_{\text{RT}}$  of the  $\text{Yb}_x\text{Y}_{1-x}\text{InCu}_4$  (filled squares) versus  $x$ .

comes from three facts. First, to meet the experimental value  $a = 0.7158$  nm for  $\text{YbInCu}_4$ . Second, the choice has to fit the experimental data of  $a$ . Third, the choice of  $a_{\text{Yb}^{+2}}$  and  $a_{\text{Yb}^{+3}}$  together with  $a_{\text{Y}}$  has to reflect the relative sizes of the ionic radii  $r(\text{Yb}^{+2}) > r(\text{Y}^{+3}) > r(\text{Yb}^{+3})$ .<sup>10</sup> We note that the radius of the  $\text{Yb}^{+2}$  ion is larger than the radius of the  $\text{Y}^{+3}$  ion and this fact explains the faint, but clear maximum at about  $x = 0.1$  (Fig. 1). This maximum cannot be achieved within the assumption that there is a difference between nominal and actual concentration of the Yb ion and that only the  $\text{Yb}^{+3}$  ions are present in an alloy. Successfully fitting the lattice parameter data allow us to conclude that our assumption is correct: in the  $\text{Yb}_x\text{Y}_{1-x}\text{InCu}_4$  alloy system there is a mixture of  $\text{Yb}^{+3}$  and  $\text{Yb}^{+2}$ , i.e., a mixed valence state, with concentrations  $C/C_{\text{th}}x$  of the magnetic ions  $\text{Yb}^{+3}$ . We speculate that the distribution of  $\text{Yb}^{+3}$  and  $\text{Yb}^{+2}$  may arise from local strain due to proximity to Y ions. Direct local structure and valence measurements would be useful in confirming this hypothesis.

In Fig. 6 we show room temperature resistivity data  $\rho_{\text{RT}}$  (closed squares). Results of measurements of (absolute) resistivity are often different from laboratory to laboratory and even from batch to batch and, moreover, from sample to sample. The main reason for this is differences in sample preparation and hence metallurgical characteristics (porosity, for example). For  $\text{YInCu}_4$  we obtain  $345 \mu\Omega \text{ cm}$  which is about 30% higher than  $247 \mu\Omega \text{ cm}$  measured by Nakamura *et al.*<sup>9</sup> Our value for  $\text{LuInCu}_4$ ,  $65 \mu\Omega \text{ cm}$ , is also 30% higher than Nakamura's one,  $40 \mu\Omega \text{ cm}$ , which shows a certain consistency. On the other hand, Müller *et al.* reported  $85 \mu\Omega \text{ cm}$  for  $\text{LuInCu}_4$ .<sup>11</sup> The value of the resistivity for  $\text{YbInCu}_4$ ,  $150 \mu\Omega \text{ cm}$ , measured by Cornelius *et al.* on samples of the same origin as ours is in good agreement with our value  $153 \mu\Omega \text{ cm}$ .<sup>3</sup> In any case we observe that the room temperature resistivities  $\rho_{\text{RT}}$  as well as the resistivities at 2 K (open squares)  $\rho_0$  are rather high, especially for low  $x$ , indicating possible semimetallic character of the  $\text{Yb}_x\text{Y}_{1-x}\text{InCu}_4$  alloys. The rather small difference between

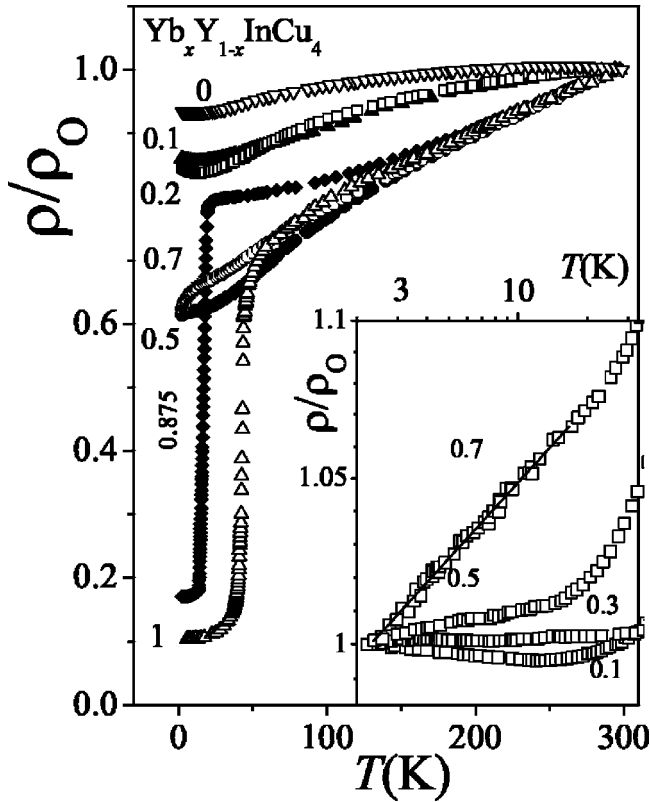


FIG. 7. The resistivity  $\rho$  of the  $\text{Yb}_x\text{Y}_{1-x}\text{InCu}_4$  alloy system for various  $x$  versus temperature  $T$ . For the sake of clarity we do not show all the measured concentrations. Inset: Some selected resistivity curves in the low temperature region. The line on the  $x=0.7$  data suggests  $+\ln T$  behavior.

the values of the resistivity at 50 K (open circles) and  $\rho_0$  for each concentration in the scale of Fig. 4 suggests that the value at 50 K could roughly represent “the residual resistivity of the high temperature phase of  $\text{Yb}_x\text{Y}_{1-x}\text{InCu}_4$ .” The concentration dependence of  $\rho_{\text{RT}}$  is quite different than that of, for example,  $\text{Ce}_x\text{La}_{1-x}\text{Cu}_{2.05}\text{Si}_2$  and  $\text{Ce}_x\text{Y}_{1-x}\text{Cu}_{2.05}\text{Si}_2$ ,<sup>12,13</sup> where  $\rho_{\text{RT}}$  increases with increasing concentration of moment bearing ion (Ce). Exponential-like decrease of  $\rho_{\text{RT}}$  is similar to the observed  $\rho_{\text{RT}}$  behavior of  $\text{Gd}_x\text{Lu}_{1-x}\text{InCu}_4$ , but there the highest resistivity is seen in  $\text{GdInCu}_4$ , which is a magnetic compound. Nevertheless, the high residual resistivity,  $350 \mu\Omega \text{ cm}$ , of  $\text{GdInCu}_4$  is not ascribed to the magnetic moment on Gd, but to the band structure of  $\text{Gd}_x\text{Lu}_{1-x}\text{InCu}_4$ .<sup>14</sup>

Another sign of a semimetallic-like band structure in the  $\text{Yb}_x\text{Y}_{1-x}\text{InCu}_4$  alloys can be seen in the temperature dependence of resistivity  $\rho(T)$  of  $\text{YInCu}_4$  (Fig. 7). The maximum at 245 K could arise from following picture. From band calculations for  $\text{LuInCu}_4$  it follows that the Fermi surface consists of a hole and an electron band with the Fermi energies  $\epsilon_F^h=0.192 \text{ eV}$  and  $\epsilon_F^e=0.592 \text{ eV}$  around  $W$  and  $X$  symmetry points, respectively.<sup>15</sup> With increasing lattice parameter band overlap and the Fermi energies should decrease. Thus for  $\text{YInCu}_4$   $\epsilon_F^h$  might be of the order of room temperature. For  $k_B T > \epsilon_F^h$  the resistivity is dominated by thermally excited carriers from some levels just below the Fermi level giving

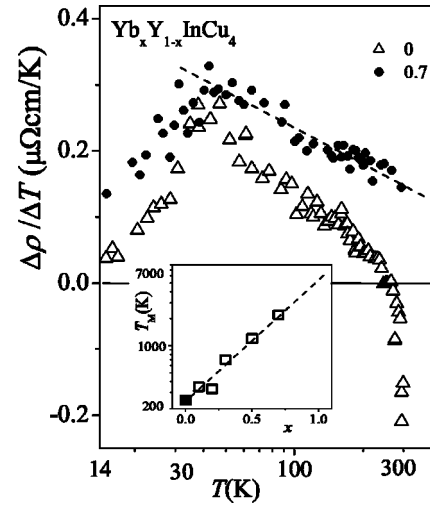


FIG. 8. The derivative of resistivity  $\Delta\rho/\Delta T$  of the  $\text{Yb}_x\text{Y}_{1-x}\text{InCu}_4$  alloy system versus  $T$ . For the sake of clarity we display only the results for  $x=0$  and  $x=0.7$ . Inset: The estimated temperature of the maximum of the resistivity  $T_M$  versus  $x$ .

rise to a semiconductor-like behavior of resistivity. Therefore, a maximum in resistivity appears roughly at  $T_M \approx \epsilon_F^h/k_B$ . For  $x=0.1$ , the maximum in the resistivity is above room temperature. However, from the derivative of the resistivity, Fig. 8, we conclude that the temperature of the maximum increases with  $x$ . Extrapolation of the data at higher temperature towards zero value at high temperatures indicates such a conclusion. The procedure is displayed for  $x=0.7$ . The estimated maxima  $T_M$  versus  $x$  are given in the inset to Fig. 8. It is interesting that the estimated maximum for  $x=0.2$  is at a lower temperature than the maximum of the  $x=0.1$  resistivity curve. The complicated concentration behavior at low  $x$  is likely caused by two competing effects. The lattice parameter increases going from  $x=0$  to  $x=0.1$ . This effect decreases overlapping between the bands and therefore  $\epsilon_F^h$  decreases. On the other hand, the presence of  $\text{Yb}^{+2}$  decreases  $\epsilon_F^e$  and  $\epsilon_F^h$  increases. Linear extrapolation of the data displayed in the inset to Fig. 8 suggests that the band width of holes of  $\text{YbInCu}_4$  is about 5000 K. From these considerations we conclude that  $\text{Yb}_x\text{Y}_{1-x}\text{InCu}_4$  assumes characteristics of compensated semimetals and that the system becomes more metallic with increasing  $x$ .

At low temperatures for the lowest concentrations only,  $x=0.1$  and  $0.2$ , there is a small logarithmic-like upturn in the resistivity (Fig. 7). As it seems small one must ensure that these upturns are intrinsic. We have calculated the slopes of the logarithmic upturn in  $\mu\Omega \text{ cm}$  per decade of temperature interval and per concentration of Yb,  $b/c$ . For  $x=0.1$   $b/c$  is  $16.45 \mu\Omega \text{ cm/mole-Yb}$  and for  $x=0.2$   $b/c$  is about  $17.5 \mu\Omega \text{ cm/mole-Yb}$ . The scatter of the slopes from the mean value is about 3%.  $b$  apparently scales with nominal concentration. The scaling is supported by the fact that the minimum of the resistivity is about the same temperature 12.5 K for both alloys. Within older theories of the Kondo problem one expects that in the single impurity regime the Kondo temperature should be independent of concentration. We calculate also  $b/c$  taking the concentration of the  $\text{Yb}^{+3}$

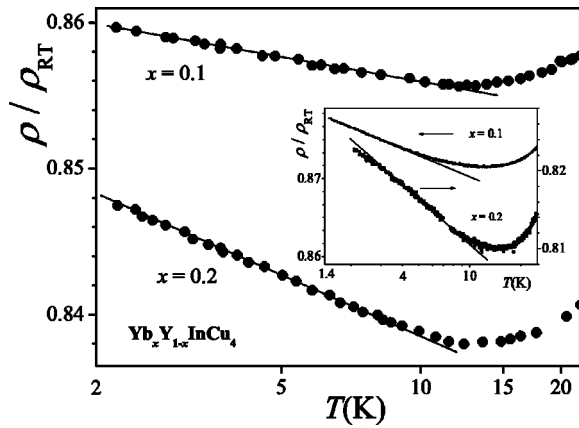


FIG. 9. The low-temperature dc resistivity of  $\text{Yb}_{0.1}\text{Y}_{0.9}\text{InCu}_4$  and  $\text{Yb}_{0.2}\text{Y}_{0.8}\text{InCu}_4$  from 2.2 K. Inset: The low temperature ac resistivity performed on the same samples down to 1.5 K.

obtained from the susceptibility measurements. The scattering from the mean slope  $53 \mu\Omega \text{ cm/mole-Yb}^{+3}$  here is greater, about 5%. However, in both cases it is less than 10%, which is the error in determination of resistivity at room temperature due to the uncertainty in determination of geometrical factor. Therefore, this experimental fact does not allow us to conclude if our assumption that the  $\text{Yb}^{+3}$  concentration in an alloy is less than the nominal concentration. However, it is likely that these upturns are of intrinsic origin. These upturns seem small in Fig. 7. However, calculated in  $\mu\Omega \text{ cm/mole-Yb}$  they are comparable to the Kondo upturn in  $\text{YbAg}_{0.6}\text{In}_{0.4}\text{Cu}_4$ ,  $42 \mu\Omega \text{ cm/mole-Yb}$ . This alloy can be treated within a single site picture and the nominal concentration represents the concentration of the  $\text{Yb}^{+3}$  ions.<sup>16</sup> In  $\text{YbCu}_3\text{Al}_2$  the slope is  $27 \mu\Omega \text{ cm/mole-Yb}$ .<sup>17</sup> In order to make a comparison we note that the value  $b/c$  for the  $\text{Ce}^{+3}$  ion in  $\text{Ce}_x\text{La}_{1-x}\text{Cu}_{2.05}\text{Si}_2$  in the impurity limit is  $185 \mu\Omega \text{ cm/mole-Yb}$ .<sup>12</sup> In the inset to Fig. 9 we present ac resistivity measurements down to 1.5 K, which extend the dc data to lower temperature.

A minimum in resistivity is sometimes taken as an estimate of the Kondo temperature. However, the position of minimum strongly depends on the high temperature contribution to resistivity. We believe that 12.5 K overestimates the Kondo temperature for  $x=0.1$  and 0.2 because in that case one should expect Kondo saturation in resistivity above 2 K. Our data do not show saturation neither in the resistivity nor in the susceptibility. We do not ascribe the bending of  $x=0.2$  below 2 K seen in the ac resistivity data (inset to Fig. 9) to Kondo saturation, but rather to intersite interactions as we shall discuss below. Therefore, the Kondo temperature might be even below 2 K. However, from an analysis of the susceptibility data it appears that the Kondo temperature is about 2 K. The scaling of the slopes indicate that the Kondo temperatures are about the same for  $x=0.1$  and 0.2.

For  $x=0.3$  the resistivity does not show the low temperature upturn and it is constant below 25 K (inset to Fig. 7). Whether this derives from an evolution of the Kondo temperature or just indicates the need to account for phonon resistivity is difficult to determine. For  $x=0.5$  and 0.7 there is a continuous decrease of the resistivity, but we can resolve

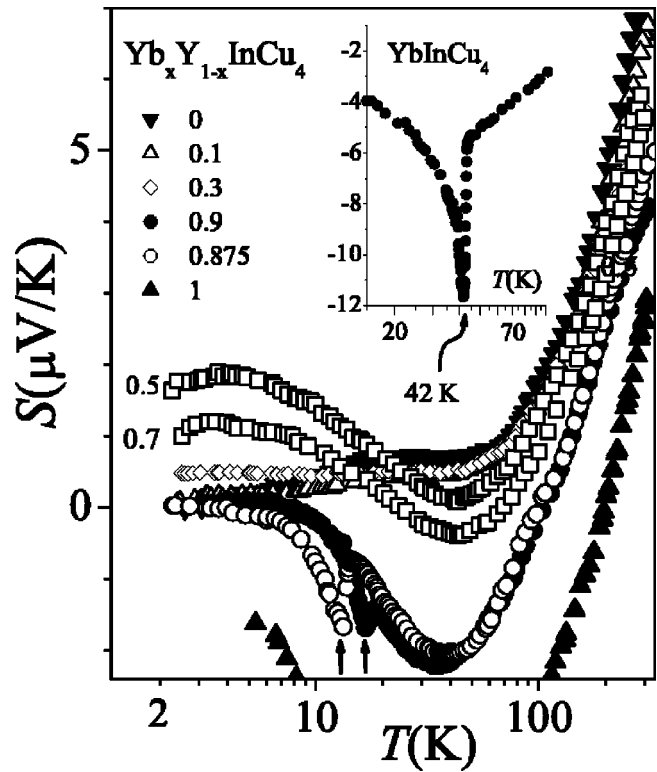


FIG. 10. The thermopower  $S$  of the  $\text{Yb}_x\text{Y}_{1-x}\text{InCu}_4$  alloy system for various  $x$  versus temperature  $T$ . By the arrows we denote the temperatures of the valence transitions for  $x=0.9$  and 0.875. For clarity we display complete thermopower of  $\text{YbInCu}_4$  in the inset.

two regimes of this decrease. Below about 15 K for  $x=0.5$  and below 25 K for  $x=0.7$  the resistivity can be described by  $+\ln T$  dependence. It is known that such a behavior of resistivity can be expected in the case of the so called inverse Kondo effect, i.e., when the coupling constant between magnetic moment and conducting electrons  $J$  would be  $>0$ . As far as we know, there are only a few systems,  $\text{FeRh}$  and  $\text{FePd}$ , that display this effect.<sup>18,19</sup> Similar temperature dependence of resistivity was found in  $\text{U}_x\text{Y}_{1-x}\text{Ru}_2\text{Si}_2$  and in  $\text{U}_x\text{Th}_{1-x}\text{Ru}_2\text{Si}_2$  ( $x < 0.08$ ).<sup>20</sup> This behavior was explained there by the two-channel Kondo effect. In that case the susceptibility should follow  $-\ln T$  behavior, which is not observed in our case. On the other hand, attempts to explain the behavior of the resistivity of  $\text{U}_x\text{Y}_{1-x}\text{Ru}_2\text{Si}_2$  ( $x=0.08$ ) due to the crystal field scattering have been made.<sup>21</sup> If we follow this approach, we should argue that the first excited state in  $\text{Yb}_{0.7}\text{Y}_{0.3}\text{InCu}_4$  is at about 20 K. However, the susceptibility investigation, which will be presented in detail elsewhere, shows that the crystal field splitting is about the same as in  $\text{YbInCu}_4$ , i.e., that the first excited crystal field level is at about 40 K.<sup>22</sup> Further, one expects a scaling with concentration of the ion if it was a single site effect. Such  $+\ln T$ -like dependence of resistivity was also reported for the  $\text{GdY}$  and  $\text{TbY}$  systems of alloys. The decrease in the resistivity there was connected with antiferromagnetic transition at low temperatures revealed by susceptibility measurement.<sup>23</sup> In our case we do not observe any magnetic phase transformation

down to 2 K for  $x=0.7$  and down to 1.5 K for  $x=0.5$ . We have examined this by ac susceptibility—not shown here. However, we note that a decrease in resistivity is usually a sign of intersite interactions. One may expect a greater contribution from intersite interaction relative to Kondo interaction with increasing  $x$  because the lattice parameter decreases. In the case of the  $\text{Yb}^{+3}$  ion one expects then a decrease of the Kondo temperature. Also, the number of the  $\text{Yb}^{+3}$  ions increases with  $x$ . Most simply, this evolution should also be reflected in the evolution of Curie-Weiss constant  $\theta$  with  $x$  in Fig. 5. That no such signature is observed suggests that multiple contributions, including Kondo and intersite interactions as well as crystal field effects, determine  $\theta$ .

Thermopower of the  $\text{Yb}_x\text{Y}_{1-x}\text{InCu}_4$  alloy system is presented in Fig. 10. At high temperatures the values of the thermopower decreases from relatively high positive values indicating possible semimetallic behavior towards lower values indicative of metallic behavior with increasing  $x$ . This general trend is consistent with the picture of the system coming from the resistivity data. However, the rate of change of the thermopower with temperature at higher temperatures for  $x=1$  is still much larger than in the case of simple metals.

Low-temperature thermopower data for low  $x$  seem to contradict the conclusions we have inferred from the resistivity. Specifically, there is no sign of Kondo behavior with the Kondo temperature about 2 K, despite the fact that thermopower is a very sensitive probe of Kondo scattering. In particular, there is no extremum in the thermopower near 2 K for  $x=0.1$  and 0.2.

In what follows we try to explain the apparently contradictory behavior of the thermopower and resistivity data at low temperatures for the lowest concentrations. From the picture of the compensated semiconductor assuming simple shaped density of the electronic states,  $g(\epsilon) \sim \epsilon^{1/2}$ , for electron and hole band, and assuming that the contributions of holes and electrons to the thermopower are additive we write the relation for thermopower

$$S = -\pi^2 k_B^2 T/3 |e| \epsilon_F^e + \pi^2 k_B^2 T/3 |e| \epsilon_F^h. \quad (3)$$

From this relation we can calculate  $\epsilon_F^e$ . In this calculation we take the value of  $S$  below 50 K to insure that the band edge effect of the hole band does not contribute significantly to the thermopower, as we believe that just this effect leads to relatively large thermopower at high temperatures. Taking  $\epsilon_F^h/k_B = 300$  K we get  $\epsilon_F^e/k_B = 320$  K in order to get the thermopower of about 1  $\mu\text{V/K}$  at 20 K consistent with the measured value for  $\text{YInCu}_4$ . Although both values  $\epsilon_F^h$  and, especially,  $\epsilon_F^e$  are certainly underestimated, this simple calculation explains some details of the data. First, we can conclude that we are dealing with compensated semimetals. If one assumed that there was effectively only one band at the Fermi level for such small value of  $\epsilon_F$  coming from resistivity data, one would get a large thermopower 20  $\mu\text{V/K}$  at 20 K. The compensated semimetallic character of  $\text{YInCu}_4$  is in line with the calculations of electronic structure of

$\text{LuInCu}_4$ .<sup>15</sup> The lattice parameter of  $\text{YInCu}_4$  is larger than that of  $\text{LuInCu}_4$ . This means that the band overlap and the Fermi energies decrease, and therefore the estimated values of  $\epsilon_F$  are lower for  $\text{YInCu}_4$  than for  $\text{LuInCu}_4$ . We note also that the number of electron carriers in  $\text{YInCu}_4$  is more than 10 times lower than in  $\text{LuInCu}_4$ .<sup>9</sup> As thermopower distinguishes sign of current carriers and is positive for holes and negative for electrons, it is likely that Kondo contributions cannot be seen in thermopower in a compensated semimetal matrix. On the other hand, in expressions for resistivity the charge of current carriers comes as  $e^2$  and thus resistivity can show Kondo scattering, as is seen for the lowest concentrations of Yb. If one supposes that the contributions of electrons and holes have to be treated as a parallel connection of two voltage sources, the discussion has to include the electron and hole conductivities. However, the main conclusion would remain the same: one may expect the absent of Kondo characteristics in thermopower due to different signs of electron and hole contributions.

It is interesting that there is a maximum in the thermopower at about 3 K for  $x > 0.3$  and  $x \leq 0.7$  where there is no sign of ordinary Kondo effect in the resistivity data. This peak could be a precursor of a magnetic ordering at lower temperatures. Similar thermopower features in Yb containing alloys and intermetallics are explained in this manner.<sup>5,24</sup> If we accept such a view, then the interpretation of this feature in the thermopower data is consistent with our interpretation of the resistivity data at those temperatures for  $x \geq 0.3$  and  $x \leq 0.7$ . We note also that one expects a minimum, not a maximum, if Kondo scattering was responsible for this extremum.<sup>4,16</sup> The minimum in thermopower data, which could be a sign of Kondo scattering, that appears at about 30 K for  $x > 0.3$  cannot be associated with the ordinary Kondo effect because there is no sign of the Kondo scattering at these temperatures in the resistivity data. Also, in the susceptibility data one should observe then either saturation or a hump as in Ref. 6.

The valence transition is detected for  $x > 0.85$  by thermopower as well as by susceptibility and resistivity data although the transition, except for  $x=1$  (inset to Fig. 10), is not so evident. A detailed study of this region will be given elsewhere, as it is beyond the scope of the current study.

#### IV. CONCLUSIONS

We report, as far as we know, the first comprehensive investigation of the  $\text{Yb}_x\text{Y}_{1-x}\text{InCu}_4$  alloy system. With increasing  $x$  the system evolves from semimetallic towards more metallic behavior. Some anomalous properties, such as the concentration dependence of the lattice parameter, which does not follow Vegard's law, can be explained by mixing of the  $\text{Yb}^{+3}$  and  $\text{Yb}^{+2}$  ions. We determine the concentration of  $\text{Yb}^{+3}$  from dc susceptibility data by an analysis of the Curie-Weiss law. Only for the lowest concentrations of Yb, we do observe sign of the Kondo effect in the resistivity data with  $T_K$  about 2 K, which is much lower than expected. Also, the Kondo contribution with such small  $T_K$  can be inferred from the dc susceptibility data. The absence of a signature of the

Kondo effect in the thermopower data for the lowest concentrations is explained by the semimetallic character of the  $\text{YInCu}_4$  matrix. The low temperature resistivity as well as the thermopower data for  $x \geq 0.3$  and  $x \leq 0.7$  show some

characteristics of the onset of intersite interaction although there is no sign of a phase transition down to 1.5 K. The valence transition is detected for  $x > 0.85$  by thermopower as well as by susceptibility and resistivity data.

\*Electronic address: ocko@ifs.hr

- <sup>1</sup>J.L. Sarrao, C.D. Immer, C.L. Benton, Z. Fisk, J.M. Lawrence, D. Mandrus, and J.D. Thompson, *Phys. Rev. B* **54**, 12 207 (1996).
- <sup>2</sup>J.L. Sarrao, *Physica B* **259–261**, 128 (1999).
- <sup>3</sup>A.L. Cornelius, J.M. Lawrence, J.L. Sarrao, Z. Fisk, M.F. Hundley, G.H. Kwei, J.D. Thompson, C.H. Booth, and F. Bridges, *Phys. Rev. B* **56**, 7993 (1997).
- <sup>4</sup>E. Bauer, *Adv. Phys.* **40**, 417 (1991).
- <sup>5</sup>K. Alami-Yadri, H. Wilhelm, and D. Jaccard, *Eur. Phys. J. B* **6**, 5 (1998).
- <sup>6</sup>W.M.C. Mattens, P.F. de Chatel, A.C. Moleman, and F.R. de Boer, *Physica B* **96**, 138 (1979).
- <sup>7</sup>M. Očko, Dj. Drobac, J.L. Sarrao, and Z. Fisk, *Phys. Rev. B* **64**, 085103 (2001).
- <sup>8</sup>M. Očko and J.L. Sarrao, *Physica B* **312–313**, 341 (2002).
- <sup>9</sup>H. Nakamura, K. Ito, and M. Shiga, *J. Phys.: Condens. Matter* **6**, 9201 (1994).
- <sup>10</sup>Web Elements™ Periodic table, <http://www.webelements.com>
- <sup>11</sup>H. Müller, E. Bauer, E. Gratz, K. Yoshimura, T. Nitta, and A. Mekata, *J. Magn. Magn. Mater.* **76–77**, 291 (1988).
- <sup>12</sup>M. Očko, D. Drobac, B. Buschinger, C. Geibel, and F. Steglich, *Phys. Rev. B* **64**, 195106 (2001).
- <sup>13</sup>M. Očko, C. Geibel, and F. Steglich, *Phys. Rev. B* **64**, 195107 (2001).
- <sup>14</sup>H. Nakamura, K. Ito, and M. Shiga, *J. Phys.: Condens. Matter* **6**, 6801 (1994).
- <sup>15</sup>K. Takegahara and T. Kasuya, *J. Phys. Soc. Jpn.* **59**, 3299 (1990).
- <sup>16</sup>M. Očko, J. L. Sarrao, and E. D. Bauer (unpublished).
- <sup>17</sup>D.P. Rojas, L.P. Cardoso, A.A. Coetho, F.G. Gandra, and A.N. Medina, *Phys. Rev. B* **63**, 165114 (2001).
- <sup>18</sup>B. R. Coles, J. H. Waszink, and J. Loram (unpublished).
- <sup>19</sup>M.P. Sarachik, *Bull. Am. Phys. Soc.* **12**, 348 (1967).
- <sup>20</sup>H. Amitsuka, K. Kuwahara, T. Yoshida, K. Tenya, T. Sakakibara, M. Mihalik, and A.A. Menowsky, *Physica B* **259–261**, 412 (1999).
- <sup>21</sup>M. Očko, J.-G. Park, and I. Aviani, *Physica B* **259–261**, 260 (1999).
- <sup>22</sup>I. Aviani, J. L. Sarrao, and M. Očko (unpublished).
- <sup>23</sup>T. Sugawara, *J. Phys. Soc. Jpn.* **20**, 2252 (1965).
- <sup>24</sup>D. Andreica, K. Alami-Yadri, D. Jaccard, A. Amato, and A. Schenck, *Physica B* **259–261**, 144 (1999).